

## Activating the Prolactin Receptor: Effect of the Ligand on the Conformation of the Extracellular Domain

Flora S. Groothuizen,<sup>†,§</sup> David Poger,<sup>†</sup> and Alan E. Mark\*,<sup>†,‡</sup>

*School of Chemistry and Molecular Biosciences, The University of Queensland, Brisbane, QLD 4072, Australia, and Institute for Molecular Bioscience, The University of Queensland, Brisbane, QLD 4072, Australia*

Received July 16, 2010

**Abstract:** The prolactin receptor resides on the surface of the cell as a preformed dimer. This suggests that cell signaling is triggered by conformational changes within the extracellular domain of the receptors. Here, by using atomistic molecular dynamics simulations, we show that the removal of the ligand placental lactogen from the dimeric form of the prolactin receptor results in a relative reorientation of the two extracellular domains by 20–30°, which corresponds to a clockwise rotation of the domains with respect to each other. Such a mechanism of activation for the prolactin receptor is similar to that proposed previously in the case of the growth hormone receptor. In addition to the effect of the removal of the ligand, the mechanical coupling between the extracellular and transmembrane domains within a model membrane was also examined.

### 1. Introduction

The prolactin (PRL) receptor (PRLR) regulates the production of milk in mammals and is involved in physiological functions, ranging from fetal growth to the regulation of hormonal balance and development of the reproductive system.<sup>1</sup> It is a class I cell surface cytokine receptor, a family that also includes the growth hormone receptor (GHR), the erythropoietin receptor (EpoR), and several interleukin receptors.<sup>2</sup> Three ligands that are similar in sequence and in their four- $\alpha$ -helix bundle structure are known to bind to PRLR: prolactin, growth hormone (GH), and placental lactogen (PL). The three PRLR-binding ligands have several overlapping functions in the body, and their metabolic states are interdependent and tightly regulated in mammals during pregnancy.<sup>3</sup>

The full-length 68.6 kDa PRLR consists of 592 amino acids, of which 210 form the N-terminal extracellular domain (ECD) that is connected to a 358-residue intracellular domain

(ICD) by a single-pass transmembrane (TM) helix of 24 amino acids. Alternative splicing of the PRLR gene results in multiple isoforms,<sup>4</sup> of which the full-length receptor is generally termed the long form.<sup>5</sup> The long form of PRLR mainly exerts its activity via the JAK2/STAT5 pathway, starting a cascade of tyrosine phosphorylations that eventually leads to the activation of target genes. The functions of the other isoforms remain uncertain, although one isoform termed the short form, containing a shorter ICD (57 residues), has been reported to have an inhibitory effect on the activity of the long form.<sup>6,7</sup>

The structure of the ECD of the long form of the PRLR has been determined as a single receptor bound to GH<sup>8</sup> or to a PRL antagonist.<sup>9</sup> However, consistent with other class I cytokine receptors, the active form of the PRLR is assumed to be a homodimer that binds its ligand in a 2:1 ratio. A crystal structure of the homodimeric rat prolactin receptor (rPRLR) ECD in complex with ovine placental lactogen (oPL) has been published.<sup>10</sup> Note that a cross-species PRLR-complex was used as the proteins in this complex can have higher affinities for each other than in the same-species complexes, which only exist transiently.<sup>11</sup> Despite the ECDs of GHR and PRLR being only ~30% identical in sequence, the tertiary structures of the PRLR ECD and GHR ECD are very similar.<sup>12</sup> Both consist of two fibronectin type III (FN-III) domains [an N-terminal domain (named D<sub>N</sub>) residues

\* Corresponding author phone: +61 7 3365 4180; fax: +61 7 3365 3872; e-mail: a.e.mark@uq.edu.au.

† School of Chemistry and Molecular Biosciences.

‡ Institute for Molecular Bioscience.

§ Present address: Division of Biochemistry and Center for Biomedical Genetics, Netherlands Cancer Institute, Plesmanlaan 121, 1066 CX Amsterdam, The Netherlands.

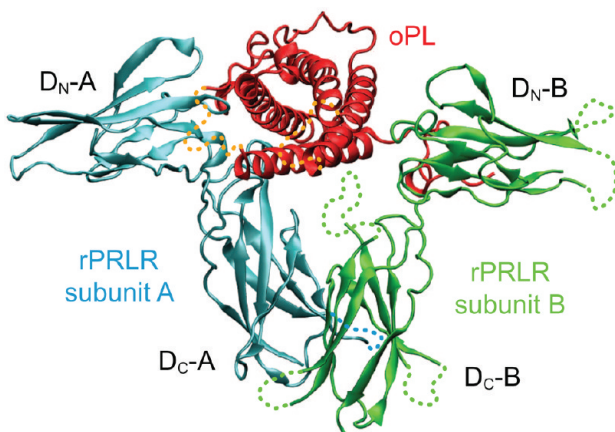


**Figure 1.** Crystal structure (Protein Data Bank entry 1F6F) of the extracellular domain of the homodimeric prolactin receptor (cyan and green) bound to placental lactogen (red) shown as a cartoon.<sup>10</sup> Each receptor subunit consists of two FN-III domains ( $D_N$  and  $D_C$ ) connected by a short hinge. Missing loops are shown as dotted lines.

Gln1–Asp96) and a C-terminal domain ( $D_C$ , residues Val101–Asp210) connected by a four-residue hinge (Val97–Ile100). The dimer (consisting of subunits A and B) is stabilized through interactions between the two C-terminal domains of each receptor subunit (termed  $D_C$ -A and  $D_C$ -B). The ligand that binds asymmetrically is primarily associated with the two N-terminal domains (termed  $D_N$ -A and  $D_N$ -B), as shown in Figure 1.

The key event in the activation of PRLR had been hypothesized to be a ligand-induced homodimerization that assumes that PRLR is predominantly monomeric on the surface of the cell<sup>13</sup> (Figure 2a). However, recent experiments such as yeast two-hybrid studies and immunoprecipitation studies suggest that, on the surface of cells, PRLR is present as a constitutive dimer even in the absence of a ligand.<sup>6</sup> More generally, the mechanism of activation of class I cytokine receptors remains unclear. If the receptor resides on the surface of cells as a preformed dimer, then the collection or cross-linking of individual receptor molecules by a ligand is unlikely to be the primary mechanism of activation. Activation could instead involve ligand-induced conformational changes within the ECD that would, in turn, induce the transmission of a mechanical signal through the plasma membrane, via the TM helices. Different motions that could give rise to activation are illustrated in Figure 2b–d. These include a translational motion (Figure 2b), a rotational motion (Figure 2c), and/or a scissor-like motion (Figure 2d) that would change the angle or the distance between the TM helices and, as a consequence, trigger changes in the orientation of the associated intracellular kinases.

In the case of GHR, a rotation of the individual ECDs within the GHR dimer has been proposed as the primary mechanism of activation.<sup>14</sup> This result has also been supported in recent simulation studies.<sup>15</sup> Specifically, atomistic molecular dynamics simulations of the GHR ECD were performed in the presence and absence of GH. Removal of GH from the crystal structure of the GH-bound GHR ECD dimer resulted in a rotation of the receptor subunits relative to each other by an angle of 45° on average, in close

agreement with experimental results in both direction and magnitude. In this study, atomistic molecular dynamics simulations have been used to investigate the mechanism of activation of PRLR, which is structurally similar to GHR. Starting from the crystal structure of the activated (hormone-bound) form of the receptor (PL-PRLR<sub>2</sub>),<sup>10</sup> a series of simulations have been conducted with and without PL. The effect of counterions and the inclusion of regions of the protein not observed in the initial crystal structure were also examined. Analysis of the structural changes within the receptor dimer consecutive to the removal of the ligand suggests a modification in the relative orientation of the extracellular domains consistent with a scissor-like mechanism. In addition, the interaction of the ECDs with a model phospholipid bilayer and the coupling of the ECDs with the TM domains were also studied.

## 2. Methods

**2.1. Simulation of the Soluble Receptor Extracellular Domain.** To examine the effect of ligand binding on the conformation of the ECD of PRLR, the ECD was simulated in water in the presence and absence of the ligand oPL. The coordinates of the 2:1 ternary complex of the rPRLR bound to oPL were taken from the structure of ref 10 [Protein Data Bank (PDB) entry 1F6F]. To assess the extent to which the loop regions that are disordered, thus not observed, in the crystal structure affect the structural stability of the domains in the receptor molecules, two systems were constructed. In the first system, only those residues present in the crystal structure were included in the model. This results in gaps in the sequence. To minimize the effects of these gaps, the amino acids preceding or following a missing residue were capped with a neutral C-amide or N-acetyl group. The residues missing included Gly48–Lys56, Ser107–Ser111, Glu198, and Thr199 of oPL; Gln1–Pro4, Gln115–Asp118, and Asn204–Asp210 in subunit A of the PRLR dimer; and Gln1–Gly5, Asp29–Pro33, Asn83–Ser87, Gln115–Lys119, Thr131–Phe140, Pro150–Glu154, and Asp205–Asp210 in subunit B of the PRLR dimer. In the second system, the missing residues were modeled using SwissPDB Viewer version 4.0.<sup>16</sup> Specifically, possible loop geometries were identified on the basis of loops in the PDB with similar sequences and a geometry chosen that had a low conformational energy and did not overlap with other atoms in the protein.

To obtain the oPL-free form of the PRLR dimer, we removed oPL from the ternary complex in both systems. In addition to the effect of modeling the missing residues, the effect of salt concentration was also examined. Each of the four systems was simulated in pure water and in the presence of a physiological salt concentration via replacement of some water molecules in the hydrated systems with Na<sup>+</sup> and Cl<sup>−</sup> ions, according to the most favorable electrostatic potential, to give a final salt concentration of 150 mM NaCl.

For the sake of simplicity, the systems that contain the bound oPL will be named with the letter B (bound) whereas the systems from which oPL has been removed will be named with the letter U (unbound). The inclusion of the

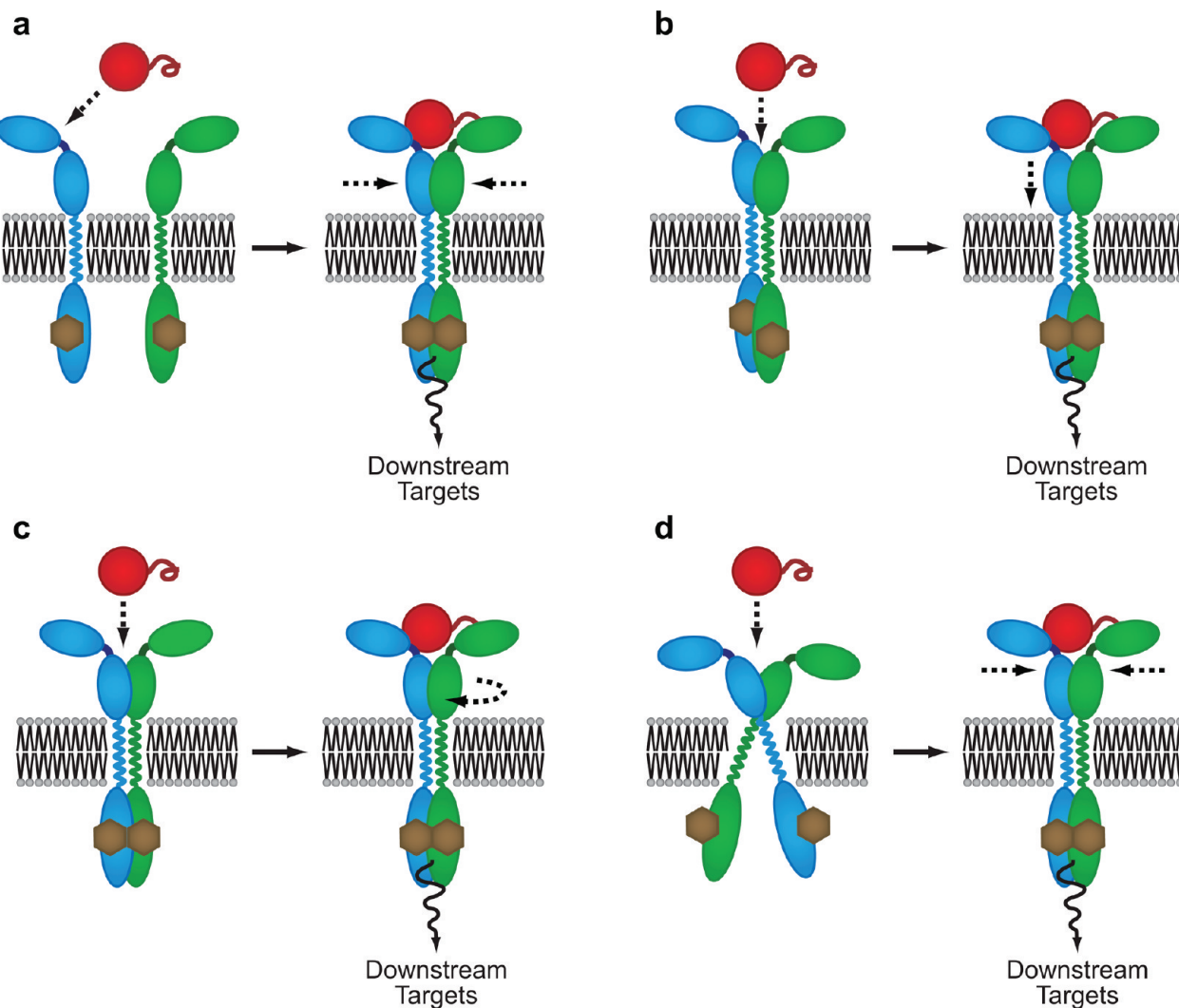


**Figure 2.** Schematic views of possible motions that may be involved in the activation of the prolactin receptor. Receptor subunits are colored blue and green, and the ligand is colored red. The brown hexagons represent kinases associated with the ICDs of the receptor subunits. (a) Ligand-induced homodimerization. A ligand binds first to one receptor molecule after which a second receptor molecule binds to form the ternary complex. (b–d) Activation of the preformed receptor dimer induced by ligand binding through (b) a translational motion, (c) a rotational motion, and (d) a scissor-like motion.

**Table 1.** Overview of the PRLR Systems That Were Simulated

system	description	[NaCl] (mM)	loops reconstructed <sup>a</sup>	lipid bilayer	linker structure <sup>b</sup>	TMD <sup>c</sup>	no. of simulations	simulation time (ns)
B	oPL-rPRLR <sub>2</sub>	0	no	no	no	no	2	37
B <sub>I</sub>	oPL-rPRLR <sub>2</sub>	150	no	no	no	no	3	37
B <sub>L</sub>	oPL-rPRLR <sub>2</sub>	0	yes	no	no	no	1	25
B <sub>LI</sub>	oPL-rPRLR <sub>2</sub>	150	yes	no	no	no	1	25
U	rPRLR <sub>2</sub>	0	no	no	no	no	6	25–58
U <sub>I</sub>	rPRLR <sub>2</sub>	150	no	no	no	no	6	18–57
U <sub>L</sub>	rPRLR <sub>2</sub>	0	yes	no	no	no	1	49
U <sub>LI</sub>	rPRLR <sub>2</sub>	150	yes	no	no	no	1	25
M <sub>R</sub>	oPL-rPRLR <sub>2</sub>	0	yes	yes	random coil	yes	1	12
M <sub>H</sub>	oPL-rPRLR <sub>2</sub>	0	yes	yes	α-helix	yes	1	10
M <sub>RA</sub>	rPRLR <sup>ΔD<sub>N</sub>D<sub>A</sub></sup>	0	yes	yes	random coil	yes	1	5.5

<sup>a</sup> Residues missing in the crystal structure: Gly48–Lys56, Ser107–Ser111, Glu198, and Thr199 of oPL; Gln1–Pro4, Gln115–Asp118, and Asn204–Asp210 in subunit A of the rPRLR dimer; and Gln1–Gly5, Asp29–Pro33, Asn83–Ser87, Gln115–Lys119, Thr131–Phe140, Pro150–Glu154, and Asp205–Asp210 in subunit B of the rPRLR dimer. <sup>b</sup> Linker region between the extracellular and transmembrane domains (residues Asp205–Asp210). <sup>c</sup> Transmembrane domain (residues Thr211–Met240). <sup>d</sup> Truncated form of the extracellular domain of PRLR from which N-terminal domain D<sub>N</sub> (residues Gln1–Asp96) has been deleted.

missing loops in the model and the presence of a physiological salt concentration will be indicated by the subscripts L and I, respectively (see Table 1).

**2.2. Simulation of the Membrane-Bound Receptor.** To study the coupling between the extracellular and transmembrane domains within the oPL-bound PRLR dimer, the two

domains were simulated in the presence of a model of the cell membrane. As the addition of the missing loops was shown to have a minor effect on the structure of the ECD of the PRL receptor and because some of the loops found to be disordered in the crystal may be involved in interactions with the plasma membrane, all missing loops were included in the model as described above. Furthermore, the C-terminal end of the ECD of each receptor subunit was extended with residues Thr211–Met240; the segment of Thr211–Leu234 has been predicted to be membrane-spanning.<sup>17</sup> Whereas the TM domain can be assumed to be helical, little is known about the structure of the six-residue linker (Asp205–Asp210) that connects the ECD of the PRLR to the TM region. The structure of this linker is, however, critical when positioning the receptor with respect to the membrane. Therefore, the linker was constructed in two alternative ways. (1) The linker was modeled as a random coil, and the ECDs were placed above the membrane (system M<sub>R</sub>). (2) The linker was modeled as a continuation of the transmembrane  $\alpha$ -helix (system M<sub>H</sub>). The objective when modeling the linker region as a random coil was to allow the system to fold spontaneously to an appropriate configuration. As this might not be possible on the time scale accessible when simulating the complete ECD dimer, a single ECD consisting of only the D<sub>C</sub> domain (rPRLR<sup>ΔD<sub>N</sub></sup>, residues Val101–Asp210) connected to a single TM region via an unstructured linker was also simulated (system M<sub>RA</sub>). In this case, the N-terminus was capped with a neutral acetyl group. In all cases, the C-terminal end of the TM domain was capped with a neutral amide group. The receptor was inserted into a fully equilibrated lipid bilayer consisting of 512 POPC (2-oleoyl-1-palmitoyl-sn-glycero-3-phosphocholine) molecules,<sup>18</sup> and the system was hydrated. The PRLR was oriented such that the long axis of the TM helices laid close to the bilayer normal, the z-axis in our coordinate system. An overview of all the PRLR systems simulated is given in Table 1.

**2.3. Simulation Parameters.** All simulations were performed using Gromacs version 3.2.1<sup>19</sup> in conjunction with the Gromos 53a6 united-atom force field.<sup>20</sup> The parameters for POPC were taken from the revised Gromos 53a6 parameter set for lipids.<sup>21</sup> Each system was subjected to periodic boundary conditions, using a truncated octahedral box for the soluble protein complexes and a rectangular box for the protein–membrane systems. The simple point charge (SPC) model<sup>22</sup> was used to describe the water. Protonation states of ionizable groups were chosen so that they were appropriate for pH 7.0.

Water, lipids, and protein were coupled separately to an external temperature bath at 298 K by using a Berendsen thermostat<sup>23</sup> with a coupling constant  $\tau_T$  of 0.1 ps. For the systems consisting of the ECD in solution (systems B, B<sub>I</sub>, B<sub>L</sub>, B<sub>LI</sub>, U, U<sub>I</sub>, U<sub>L</sub>, and U<sub>LI</sub>), the pressure was maintained at 1 bar by isotropically coupling the system to an external bath again using the method of Berendsen<sup>23</sup> with an isothermal compressibility of  $4.6 \times 10^{-5}$  bar<sup>-1</sup> and a coupling constant  $\tau_P$  of 1 ps. For those systems in which the receptor was embedded within a membrane (systems M<sub>R</sub>, M<sub>H</sub>, and M<sub>RA</sub>), semi-isotropic pressure coupling was used. The same parameter values were used for the directions normal and

parallel to the plane of the POPC bilayer as for the simulations in water.

A twin-range cutoff scheme was used for the evaluation of nonbonded interactions: interactions falling within the short-range cutoff of 0.8 nm were calculated every step, whereas interactions falling within the long-range cutoff of 1.4 nm were updated every three steps. A reaction-field correction<sup>24</sup> was applied to account for the truncation of the electrostatic interactions beyond the long-range cutoff with an  $\epsilon_{RF}$  of 78.

During the simulations, bond lengths within the solute molecules were constrained using the LINCS algorithm.<sup>25</sup> To extend the time scale that could be simulated, hydrogen atoms in the proteins were replaced with dummy interaction sites, the positions of which were constructed at each step from the coordinates of the heavy atoms to which they were attached. This allowed a 4 fs time step to be used without affecting the thermodynamic properties of the systems significantly.<sup>26</sup>

To remove possible bad contacts between atoms stemming from the original crystal structure or introduced during the modeling of the loops, the systems were first energy-minimized in vacuo and then in solution using a steepest-descent algorithm. The systems were then equilibrated by gradually increasing the temperature from 50 to 298 K in 50 K steps over a time span of 200 ps before the simulations commenced. Starting velocities were randomly assigned from a Maxwellian distribution with different random seeds for each simulation. In total, the isolated ECD of the PRLR was simulated independently seven times in the presence of oPL and 14 times after oPL was removed. Each simulation in solution was at least 18 ns in length, and configurations were saved every 10 ps for analysis.

**2.4. Analysis.** Prior to analysis, the initial structure of the receptor dimer was reoriented such that the longest axis of the D<sub>C</sub> domain of subunit A (D<sub>C</sub>-A) was aligned along the z-axis. The longest axis in the D<sub>C</sub> domains was chosen as the vector connecting the C<sub>α</sub> atoms of His188 and Pro203 in each receptor subunit. Furthermore, the axis defined by the x–y coordinates of the center of mass of the D<sub>C</sub>-A and D<sub>C</sub>-B domains was aligned along the x-axis. Then, the structures from the trajectories of the simulations were superimposed with respect to the backbone of D<sub>C</sub>-A. The relative angle of rotation  $\theta$  between the D<sub>C</sub> domains was defined as the angle between the long axis of the two D<sub>C</sub> domains when projected onto the y–z plane, as depicted in Figure 3.

The root-mean-square deviation (rmsd) of the coordinates of the backbone atoms (N, C<sub>α</sub>, C, and O) was calculated after a least-squares fit on the backbone atoms of the initial structure of every domain, subunit, or complex had been performed separately. The rmsd values for the region of interest were calculated with respect to the initial X-ray structure. For these calculations, the (N-terminal) D<sub>N</sub> domain and the (C-terminal) D<sub>C</sub> domain of a given PRLR subunit were defined by including only those residues present in the crystal structure. The D<sub>N</sub> domain comprised Gln1–Asp96 and the D<sub>C</sub> domain Val101–Asn204.

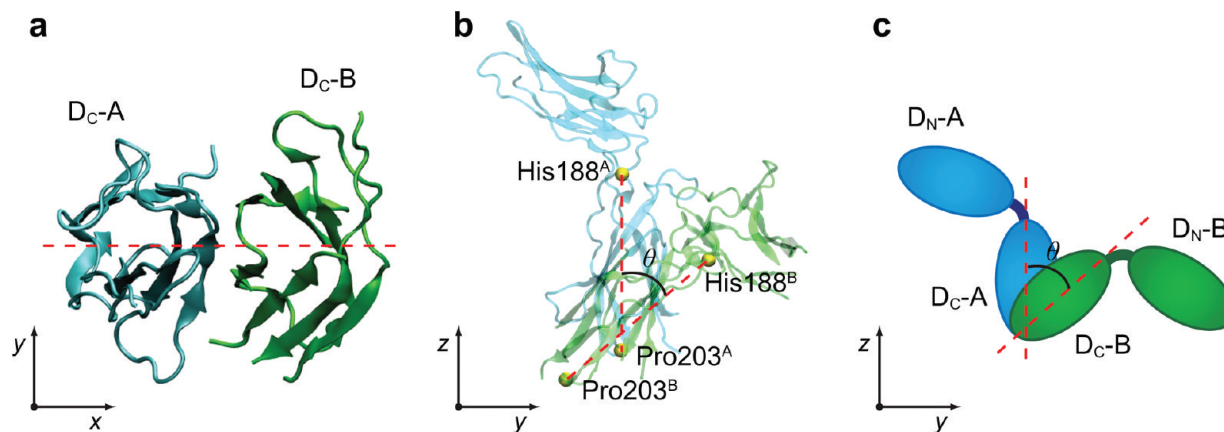


**Figure 3.** Method for measuring the angle  $\theta$  between the two  $D_C$  domains. (a) The two domains are first aligned along the  $x$ -axis. (b) The long axis of each  $D_C$  domain was taken as the vector connecting the  $C_\alpha$  atoms of His188 and Pro203 (His188<sup>A</sup> and Pro203<sup>A</sup> in subunit A and His188<sup>B</sup> and Pro203<sup>B</sup> in subunit B). This axis in subunit A is then aligned along the  $z$ -axis. The angle  $\theta$  is defined as the angle between the long axis of subunits A and B, projected onto the  $y$ - $z$  plane. (c) Schematic view of the angle  $\theta$  between the two  $D_C$  domains in the receptor dimer.

### 3. Results

**3.1. Dynamic Properties of the Isolated Receptor Complex.** We assessed the dynamics of the ternary oPL–rPRLR<sub>2</sub> complex in solution by conducting seven independent simulations of the receptor ECD with its ligand in a box of water. In five of these simulations, the model included only those residues for which coordinates were given in the X-ray crystal structure. In the two other simulations, the model was augmented to include the effect of modeling the missing loop residues. The effect of the physiological concentration of salt was also investigated. Of the five simulations that involved only those residues in the crystal structure, two were performed in pure water (simulations B-1 and B-2), while the three other were performed in the presence of 150 mM NaCl (simulations B<sub>I</sub>-1–B<sub>I</sub>-3). Of the two simulations including the modeled loops, one was performed in pure water (simulation B<sub>L</sub>-1) and one in 150 mM NaCl (simulation B<sub>L</sub>-1).

The dynamics of the homodimeric rPRLR<sub>2</sub> complex from which the ligand oPL had been removed was studied via 14 independent simulations. Of these, 12 comprised only those residues observed in the crystal structure, while in two, the missing loops were included in the model. Half of the simulations were performed in pure water (simulations U-1–U-6 and U<sub>L</sub>-1) and half in the presence of 150 mM NaCl (simulations U<sub>I</sub>-1–U<sub>I</sub>-6 and U<sub>L</sub>-1).

**3.1.1. Structural Stability.** As shown in Figure 1, the ECD of the PRLR consists of two fibronectin type III (FN-III) domains, the N-terminal domain ( $D_N$ ) and the C-terminal domain ( $D_C$ ), connected via a flexible hinge region. To examine whether the force field could maintain the structure of the protein and to examine the effect on the structural stability of the protein caused by the introduction of residues missing in the crystal structure and/or the inclusion of 150 mM NaCl, the rmsd of the positions of the backbone atoms of each domain with respect to the starting crystal structure was determined. The structure of the individual FN-III domains was stable under all conditions. The average rmsd over the last 5 ns of each simulation varied between 0.13

and 0.30 nm. The inclusion of missing amino acids in the model and/or 150 mM NaCl had no obvious effect on the stability of the individual domains (Figure 4a,b). For example, in the case of the unliganded dimer in which residues missing in the crystal structure were not included in the model, resulting in a discontinuous backbone with multiple breaks (simulations U-1–U-6), the average backbone rmsd with respect to the crystal structure was only  $0.21 \pm 0.03$  nm for both the  $D_N$  and  $D_C$  domains. Essentially identical rmsd values ( $0.19 \pm 0.04$  and  $0.20 \pm 0.05$  nm in domains  $D_N$  and  $D_C$ , respectively) were obtained in the presence of 150 mM NaCl (simulations U<sub>I</sub>-1–U<sub>I</sub>-6).

**3.1.2. Effect of the Removal of oPL from the rPRLR<sub>2</sub> Complex.** Although the structure of the individual FN-III domains was stable, significant motions between the domains were observed in all cases. The average rmsd over the last 5 ns of all the simulations of the ternary oPL–PRLR<sub>2</sub> complex was  $0.45 \pm 0.09$  nm. This was largely because of changes in the position of the oPL ligand as the rmsd of the PRLR<sub>2</sub> dimer alone was  $0.37 \pm 0.12$  nm. As the rmsd is a highly nonlinear measure, such values are easily obtained because of slight changes in the relative positions of the domains. Again, the effect of the inclusion of the missing residues or 150 mM NaCl was minor.

The removal of oPL from the ternary complex led in contrast to marked fluctuations in the overall rmsd. The large variations in rmsd with values reaching as high as 1.4–1.6 nm were a result of rigid-body hinge-bending motions within the individual subunits of the receptor dimer, as well as changes in the orientation of the two subunits with respect to each other. This type of interdomain motion is exemplified in Figure 4c, which shows the time evolution of the backbone rmsd with respect to the starting crystal structure for simulation U<sub>I</sub>-3. Figure 4d shows various snapshots from the trajectory illustrating changes in the relative position of the  $D_N$  and  $D_C$  domains. As is evident from Figure 4d, the relative motion of the domains is reversible with the subunit flexing around the hinge region, opening and then closing the ligand-binding site. Again, similar results were obtained

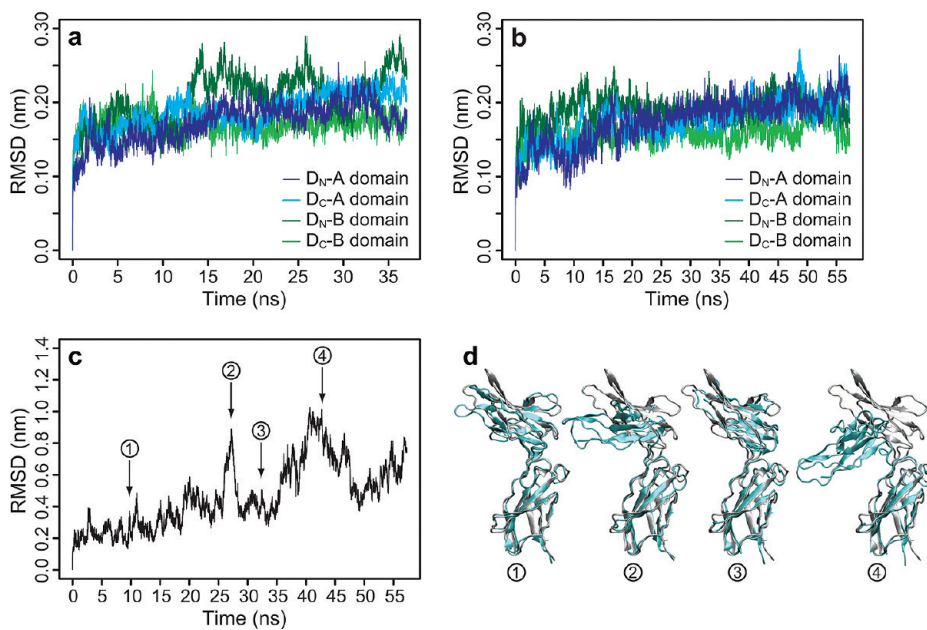


**Figure 4.** Conformational flexibility within the subunits of the prolactin receptor dimer. (a) Time evolution of the backbone rmsd calculated for the two fibronectin type III domains in subunits A and B of the oPL-bound receptor dimer in simulation B<sub>l</sub>-1 with respect to the crystal structure. (b) Time evolution of the backbone rmsd calculated for the two fibronectin type III domains in subunits A and B of the unliganded receptor dimer in simulation U<sub>l</sub>-3 with respect to the crystal structure. (c) Time evolution of the backbone rmsd of subunit B in simulation U<sub>l</sub>-3 with respect to the crystal structure. (d) Snapshots from simulation U<sub>l</sub>-3 at times corresponding to the arrows in panel c.

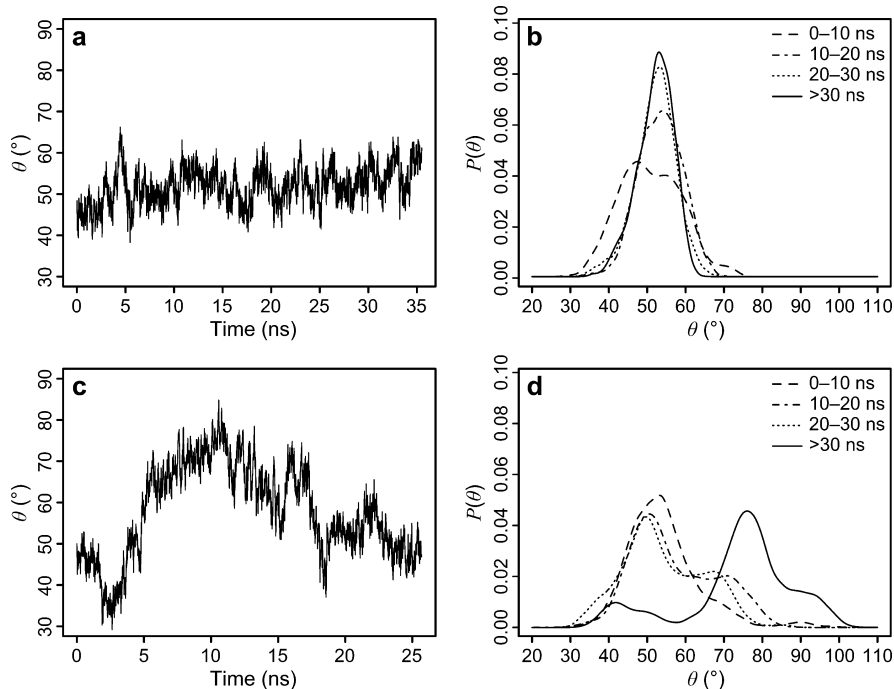


**Figure 5.** Time evolutions (a and c) and probability distributions (b and d) of the angle of rotation  $\theta$  between the long axes of the two D<sub>C</sub> domains of the subunits over the course of the simulations of the oPL-bound (a and b) and oPL-free (c and d) PRLR dimer. (a) Time evolution of  $\theta$  in simulation B<sub>l</sub>-2. (b) Probability distribution of  $\theta$  calculated over all seven ligand-bound PRLR simulations and over four time ranges. (c) Time evolution of  $\theta$  in simulation U-6. (d) Probability distribution of  $\theta$  calculated over all 14 PRLR simulations after removal of oPL and over four time ranges.

in the presence or absence of 150 mM NaCl and regardless of whether the missing residues were included in the model.

**3.2. Changes in the Relative Orientation of the Receptor Subunits.** In addition to fluctuations in the relative positions of the D<sub>N</sub> and D<sub>C</sub> domains, the removal of the oPL

ligand was associated with changes in the relative orientation of the receptor subunits. Figure 5 shows the time evolution and distribution of the angle  $\theta$  formed by the long axis of the two D<sub>C</sub> domains in simulations in the presence (panels a and b) and absence (panels c and d) of oPL. In the X-ray

structure, the long axes of the two D<sub>C</sub> domains make an angle of 49° with respect to each other. In the simulations of the oPL–PRLR<sub>2</sub> complex, the angle  $\theta$  is essentially unchanged, fluctuating around an average value of 53°. This is illustrated in Figure 5a, which shows the variation of  $\theta$  as a function of the simulation time for one of the simulations of the oPL–PRLR<sub>2</sub> complex in the presence of 150 mM NaCl (B<sub>1</sub>–2). As one can see,  $\theta$  fluctuates between 40° and 65°. Similar results were obtained in all simulations of the ternary complex. The probability distribution of the value of  $\theta$  calculated over all seven liganded simulations shows a single peak centered at 53° that becomes progressively narrower with time. In contrast, the removal of oPL from the complex resulted in large variations in the angle during the simulations. This is illustrated by the time evolution of  $\theta$  during simulation U-6 in Figure 5c. In this case, it can be seen that  $\theta$  increases to approximately 80° before falling again to around 50°. An increase in  $\theta$  is associated with a clockwise rotation of one domain relative to the other.

As is evident from Figure 5c, the change in the relative orientation of the D<sub>C</sub> domains after the removal of the oPL ligand is a stochastic process, and little can be inferred from a single simulation. However, upon combination of the results of all 14 simulations performed in the absence of oPL (Figure 5d), a bimodal behavior clearly appears, with the receptor dimer having two preferred angles: one centered between 45° and 55° and the other centered between 70° and 80°. Furthermore, there was a distinct shift as a function of time toward higher values of  $\theta$ .

As noted above, the change in the relative orientation of the D<sub>C</sub> domains is also associated with a clockwise rotation of the domains with respect to each other that, in turn, leads to an increase in the distance between their D<sub>N</sub> domains as illustrated in Figure 6. Figure 6 shows the initial and final configurations from simulation U-6. The reorientation of the D<sub>C</sub> domains results in an opening of the ligand-binding site and the exposure of the binding surfaces on the D<sub>N</sub> domains. Nonetheless, the primary hydrogen bonds and hydrophobic interactions between residues positioned at the interface of the D<sub>C</sub> domains (subunit A, mainly Phe167–Asp171; subunit B, mainly Phe160–Gln164) were maintained (Figure 6a,b). At least on the time scale of the simulations, there was no evidence to suggest that the removal of the ligand would cause the complex to dissociate.

**3.3. Interaction of the Extracellular Domain with a POPC Membrane.** A major unanswered question with regard to the mechanism of action of all class I cytokine receptors is how the extracellular domains are mechanically coupled to the transmembrane domains. If the transmission of a signal is the result of a structural change in the ECDs as has been suggested here and in previous studies,<sup>14,15,27</sup> the structure of the linker that connects the ECD to its TM helix is critical. Specifically, if the linker is to transmit a mechanical signal, then it is expected that the linker would be rigid and tightly coupled to both the ECD and the TMD. Such a coupling could occur if the linker adopted a helical or  $\beta$ -sheet structure or folded onto the ECD to lock the TMD to the receptor ECD at the surface of the membrane. As no information about the structure of the linker is available, a

series of simulations of the complete receptor complex embedded within a POPC bilayer were performed. The aim of these studies was two-fold: to attempt to shed light on the ECD–TMD coupling via the linker region and to understand the nature of the interaction of the ECD with the lipid bilayer. Several different approaches were used to model the linker region in the context of the ligand-bound receptor dimer. In the first approach (simulation M<sub>R</sub>), the linker between the ECD and the TM helix was modeled in an extended, random-coil conformation to produce an unbiased starting configuration (Figure 7a). In this case, the linker rapidly associated (within 3 ns of simulation) with residues of the base of the ECD, forming an array of hydrogen bonds and salt bridges. This resulted in the ECD interacting directly with the membrane. In particular, charged residues within the loops that were disordered in the crystal structure interacted directly with the lipid headgroups (Figure 7b). However, despite the ECD lying in the proximity of the TMD, the linker region itself did not adopt a clearly defined structure.

In the second approach (simulation M<sub>H</sub>), the linker region was modeled as a helical elongation of the transmembrane helix as depicted in Figure 7c. Such a helical linker would provide a direct way to couple changes in the relative orientation of the D<sub>C</sub> domains via the TMDs to the ICDs. Nonetheless, in this case, the helical linker immediately

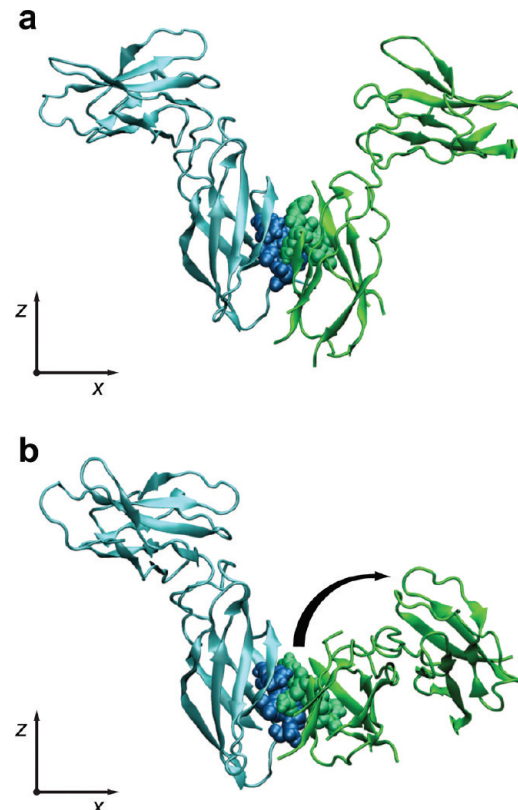


**Figure 6.** Rotation between the subunits of the rPRLR within the dimer when simulated after removal of oPL. (a) Initial structure (subunits A and B colored cyan and green, respectively) with residues that keep interacting when the subunits move with respect to each other depicted as spheres. (b) Structure after simulation for 17.5 ns with subunit B tilted backward (simulation U-1).

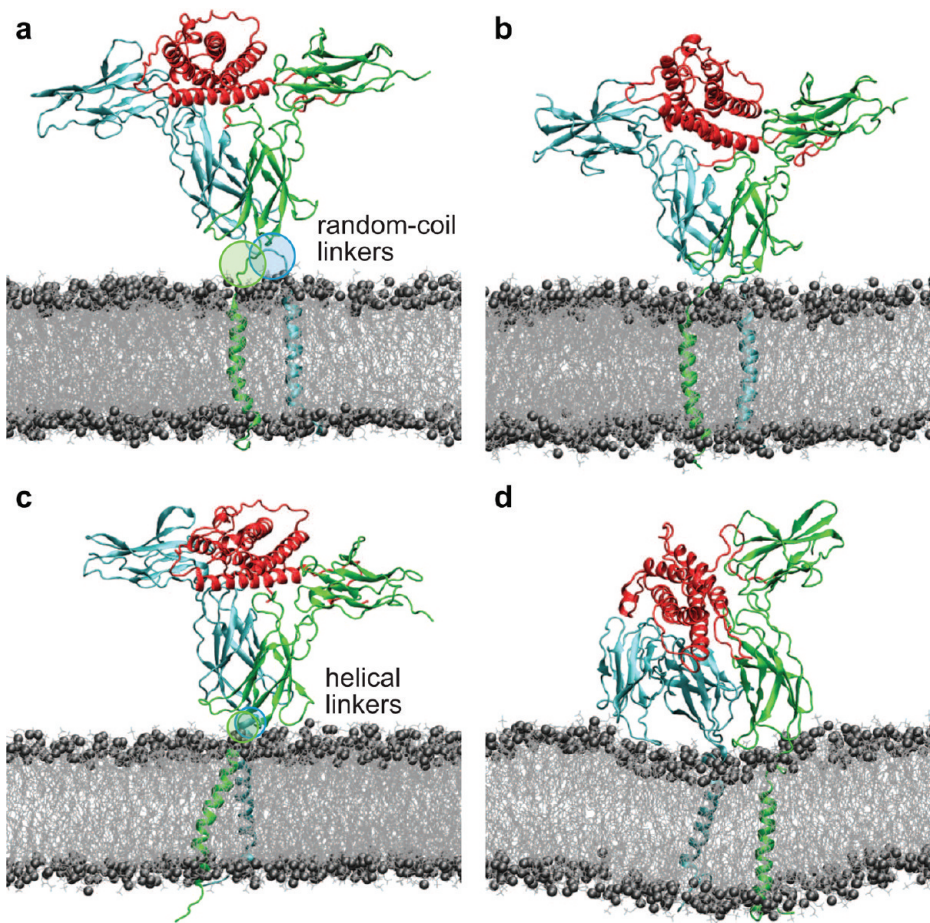


**Figure 7.** Initial and representative final configurations of simulations of the ECD and TMD of the rPRLR<sub>2</sub> dimer in a complex with oPL and embedded within a POPC bilayer performed using two different initial configurations of the linker region. (a and b) The linker region was modeled in an extended structure: (a) initial structure and (b) structure after simulation for 3 ns. (c and d) The linker region was helical: (c) initial structure and (d) structure after simulation for 9 ns. The ECDs of the rPRLR subunits are colored cyan and green, and oPL is colored red. The lipids are shown as light gray lines, and phosphorus atoms shown as dark gray spheres. The linkers are circled in cyan and green.

unfolded, and again, the base of the ECD interacted strongly with the membrane (Figure 7d). Although this does not mean the linker cannot be helical, it does imply that the structure of the receptor dimer determined in a nonphysiological environment and the arrangement in which the TMDs lie in an approximately parallel configuration are incompatible with the linker being a helical extension of the TMD.

A third system in which the D<sub>C</sub> domain of a single subunit (the D<sub>N</sub> domain of the ECD was removed) was also coupled to the TMD via a linker in an extended conformation was simulated (simulation M<sub>RA</sub>). Again, the base of the D<sub>C</sub> domain embedded in the membrane before the linker region could not fold into a specific conformation.

#### 4. Discussion

Despite many years of investigation, the precise mechanism by which the binding of a class I cytokine to the extracellular domain of its corresponding receptor transmits a signal through the cell membrane is unknown. While it is possible that activation may involve the collection of two receptor subunits by a ligand, there is growing evidence that class I cytokine receptors such as the growth hormone receptor (GHR), the erythropoietin receptor (EpoR) and the prolactin

receptor (PRLR) reside on the membrane as preformed dimers.<sup>7,28</sup> In this case, the activation of the receptor is most likely linked to the relative position or orientation of the receptor subunits, such as the relative rotation and/or translation of the subunits or a scissor-like movement of the subunits (illustrated in Figure 2b–d). In this study, we have attempted to determine which of these underlying mechanisms could lead to activation of the PRLR by examining the effect of the removal of ligand from the crystal structure of the activated complex and by examining the mechanical coupling of the ECD to the TM domain.

Our results suggest that in the absence of ligand, the receptor dimer shows a high degree of flexibility and that it can adopt two distinct conformations that differ in the relative subunit orientation of the membrane-proximal (D<sub>C</sub>) domains. Furthermore, the simulations suggest that the binding of a ligand, in this case placental lactogen, stabilizes one of these two preexisting conformations, rigidifying the complex. In this respect, ligand binding can be viewed as introducing a clockwise rigid-body rotation of one subunit with respect to the other by ~20–30°. Importantly, this was associated with only minor changes in the nature of the interactions at the interface between the two subunits. These findings indicate

that the activation mechanism for PRLR may involve changes in the relative orientation of the ECD similar to those proposed in the case of the activation of GHR in both experiment and simulation.<sup>14,15</sup> As the monomeric GHR and PRLR and their corresponding dimers are structurally very similar, it is not surprising that the simulations showed related, but slightly different, motions for the two receptors.

It has been found experimentally that the deletion of the N-terminal tail of PL greatly reduces the activity of the ligand.<sup>29</sup> From the crystal structure (Figure 1), one can see that oPL is mainly associated with the D<sub>N</sub>-A domain and only the N-terminal end of placental lactogen binds to the D<sub>N</sub>-B domain. Thus, it is likely that it is the binding of the N-terminal tail to the D<sub>N</sub>-B domain that stabilizes the rotated (activated) form of the complex.

The mechanism that we would propose is one in which in the absence of ligand, both D<sub>N</sub> domains are solvent-exposed and the ECD is predominantly in an open, inactive form. The binding of a ligand stabilizes the rotated form, leading to a change in the relative orientation of the TMDs and, thus, the relative positions of the intracellular domains.

A critical aspect of the model is the degree of mechanical coupling between the ECD and the TMD. The simulations that were performed in an attempt to address this issue suggest that the base of the D<sub>C</sub> domains of the PRLR interact significantly with the membrane as opposed to the ECD standing proud of the membrane, and that the structure of this region in the available crystal structure may not be representative of that in a physiologically relevant environment. In addition, inasmuch as the linker between the ECD and the TMD was relatively flexible and did not fold into a specific conformation in any of the simulations, the ECD and the TMD may interact directly to transmit the mechanical signal through the membrane.

In summary, we have proposed a model for activation of the prolactin receptor, taking into account the necessity for the receptor to transfer a signal through the cell membrane that involves changes in the relative orientation of the extracellular domains upon binding of a ligand. This suggests that a relative rotation of the extracellular domains may represent a general model for the activation of class I cytokine receptors. Furthermore, we have shown that the extracellular domains interact strongly with the membrane and that to understand the mechanical coupling between the extracellular and transmembrane domains, an appropriate representation of the environment of the membrane–water interface will be critical.

## Abbreviations

D<sub>C</sub>, C-terminal domain of the extracellular domain of the prolactin receptor; D<sub>N</sub>, N-terminal domain of the extracellular domain of the prolactin receptor; ECD, extracellular domain; FN-III, fibronectin type III; GH, growth hormone; GHR, growth hormone receptor; ICD, intracellular domain; oPL, ovine placental lactogen; PL, placental lactogen; POPC, 2-oleoyl-1-palmitoyl-sn-glycero-3-phosphocholine; PRL, prolactin; PRLR, prolactin receptor; rmsd, root-mean-square deviation; rPRLR, rat prolactin receptor; TM, transmembrane; TMD, transmembrane domain.

**Acknowledgment.** This work was funded by the Australian Research Council (ARC). A.E.M. is an ARC Federation Fellow. All the calculations were performed using high-performance computing resources of The University of Queensland and of the National Computational Infrastructure (NCI) National Facility at the Australian National University under the Merit Allocation Scheme through the Queensland Cyber Infrastructure Foundation (QCIF) partner share scheme.

## References

- (1) Bole-Feysot, C.; Goffin, V.; Edery, M.; Binart, N.; Kelly, P. A. Prolactin (PRL) and its receptor: Actions, signal transduction pathways and phenotypes observed in PRL receptor knockout mice. *Endocr. Rev.* **1998**, *19*, 225–268.
- (2) Bazan, J. F. Structural design and molecular evolution of a cytokine receptor superfamily. *Proc. Natl. Acad. Sci. U.S.A.* **1990**, *87*, 6934–6938.
- (3) Grattan, D. R.; Steyn, F. J.; Kokay, I. C.; Anderson, G. M.; Bunn, S. J. Pregnancy-induced adaptation in the neuroendocrine control of prolactin secretion. *J. Neuroendocrinol.* **2008**, *20*, 497–507.
- (4) Hu, Z. Z.; Zhuang, L.; Dufau, M. L. Prolactin receptor gene diversity: Structure and regulation. *Trends Endocrinol. Metab.* **1998**, *9*, 94–102.
- (5) Trott, J. F.; Hovey, R. C.; Koduri, S.; Vonderhaar, B. K. Alternative splicing to exon 11 of human prolactin receptor gene results in multiple isoforms including a secreted prolactin-binding protein. *J. Mol. Endocrinol.* **2003**, *30*, 31–47.
- (6) Gadd, S. L.; Clevenger, C. V. Ligand-independent dimerization of the human prolactin receptor isoforms: Functional implications. *Mol. Endocrinol.* **2006**, *20*, 2734–2746.
- (7) Qazi, A. M.; Tsai-Morris, C.-H.; Dufau, M. L. Ligand-independent homo- and heterodimerization of human prolactin receptor variants: Inhibitory action of the short forms by heterodimerization. *Mol. Endocrinol.* **2006**, *20*, 1912–1923.
- (8) Somers, W.; Ultsch, M.; de Vos, A. M.; Kossiakoff, A. A. The X-ray structure of a growth hormone-prolactin receptor complex. *Nature* **1994**, *372*, 478–481.
- (9) Svensson, L. A.; Bondensgaard, K.; Nørskov-Lauritsen, L.; Christensen, L.; Becker, P.; Andersen, M. D.; Maltesen, M. J.; Rand, K. D.; Breinholt, J. Crystal structure of a prolactin receptor antagonist bound to the extracellular domain of the prolactin receptor. *J. Biol. Chem.* **2008**, *283*, 19085–19094.
- (10) Elkins, P. A.; Christinger, H. W.; Sandowski, Y.; Sakal, E.; Gertler, A.; de Vos, A. M.; Kossiakoff, A. A. Ternary complex between placental lactogen and the extracellular domain of the prolactin receptor. *Nat. Struct. Biol.* **2000**, *7*, 808–815.
- (11) Gertler, A.; Grosclaude, J.; Strasburger, C. J.; Nir, S.; Djiane, J. Real-time kinetic measurements of the interactions between lactogenic hormones and prolactin-receptor extracellular domains from several species support the model of hormone-induced transient receptor dimerization. *J. Biol. Chem.* **1996**, *271*, 24482–24491.
- (12) de Vos, A.; Ultsch, M.; Kossiakoff, A. A. Human growth hormone and extracellular domain of its receptor: Crystal structure of the complex. *Science* **1992**, *255*, 306–312.
- (13) Sakal, E.; Elberg, G.; Gertler, A. Direct evidence that lactogenic hormones induce homodimerization of membrane-anchored prolactin receptor in intact Nb2-11C rat lymphoma cells. *FEBS Lett.* **1997**, *410*, 289–292.

- (14) Brown, R. J.; Adams, J. J.; Pelekanos, R. A.; Wan, Y.; McKinstry, W. J.; Palethorpe, K.; Seeber, R. M.; Monks, T. A.; Eidne, K. A.; Parker, M. W.; Waters, M. J. Model for growth hormone receptor activation based on subunit rotation within a receptor dimer. *Nat. Struct. Mol. Biol.* **2005**, *12*, 814–821.
- (15) Pogorelyak, D.; Mark, A. E. Turning the growth hormone receptor on: Evidence that hormone binding induces subunit rotation. *Proteins* **2010**, *78*, 1163–1174.
- (16) Guex, N.; Peitsch, M. SWISS-MODEL and the Swiss-PdbViewer: An environment for comparative protein modeling. *Electrophoresis* **1997**, *18*, 2714–2723.
- (17) Boutin, J.-M.; Jolicoeur, C.; Okamura, H.; Gagnon, J.; Edery, M.; Shiota, M.; Banville, D.; Dusander-Fournier, I.; Djiane, J.; Kelly, P. A. Cloning and expression of the rat prolactin receptor, a member of the growth hormone/prolactin receptor gene family. *Cell* **1988**, *53*, 69–77.
- (18) Pogorelyak, D.; Mark, A. E. On the validation of molecular dynamics simulations of saturated and *cis*-monounsaturated phosphatidylcholine lipid bilayers: A comparison with experiment. *J. Chem. Theory Comput.* **2010**, *6*, 325–336.
- (19) van der Spoel, D.; Lindahl, E.; Hess, B.; Groenhof, G.; Mark, A. E.; Berendsen, H. J. C. Gromacs: Fast, flexible, and free. *J. Comput. Chem.* **2005**, *26*, 1701–1718.
- (20) Oostenbrink, C.; Villa, A.; Mark, A. E.; van Gunsteren, W. F. A biomolecular force field based on the free enthalpy of hydration and solvation: The Gromos force-field parameter sets 53a5 and 53a6. *J. Comput. Chem.* **2004**, *25*, 1656–1676.
- (21) Pogorelyak, D.; van Gunsteren, W. F.; Mark, A. E. A new force field for simulating phosphatidylcholine bilayers. *J. Comput. Chem.* **2010**, *30*, 117–125.
- (22) Berendsen, H. J. C.; Postma, J. P. M.; van Gunsteren, W. F.; Hermans, J. Interaction models for water in relation to protein hydration. In *Intermolecular Forces*; Reidel: Dordrecht, The Netherlands, 1981; pp 331–342.
- (23) Berendsen, H. J. C.; Postma, J. P. M.; van Gunsteren, W. F.; DiNola, A.; Haak, J. R. Molecular dynamics with coupling to an external bath. *J. Chem. Phys.* **1984**, *81*, 3684–3690.
- (24) Tironi, I. G.; Sperb, R.; Smith, P. E.; van Gunsteren, W. F. A generalized reaction field method for molecular dynamics simulations. *J. Chem. Phys.* **1995**, *102*, 5451–5459.
- (25) Hess, B.; Bekker, H.; Berendsen, H. J. C.; Fraaije, J. G. E. M. LINCS: A linear constraint solver for molecular simulations. *J. Comput. Chem.* **1997**, *18*, 1463–1472.
- (26) Feenstra, K.; Hess, B.; Berendsen, H. J. C. Improving efficiency of large time-scale molecular dynamics simulations of hydrogen-rich systems. *J. Comput. Chem.* **1999**, *20*, 786–798.
- (27) Seubert, N.; Royer, Y.; Staerk, J.; Kubatzky, K. F.; Moucadel, V.; Krishnakumar, S.; Smith, S. O.; Constantinescu, S. N. Active and inactive orientations of the transmembrane and cytosolic domains of the erythropoietin receptor dimer. *Mol. Cell* **2003**, *12*, 1239–1250.
- (28) Gent, J.; van Kerkhof, P.; Roza, M.; Bu, G.; Strous, G. J. Ligand-independent growth hormone receptor dimerization occurs in the endoplasmic reticulum and is required for ubiquitin system-dependent endocytosis. *Proc. Natl. Acad. Sci. U.S.A.* **2002**, *99*, 9858–9863.
- (29) Gertler, A.; Hauser, S. D.; Sakal, E.; Vashdi, D.; Staten, N.; Freeman, J. J.; Krivi, G. G. Preparation, purification, and determination of the biological activities of 12 N-terminus-truncated recombinant analogues of bovine placental lactogen. *J. Biol. Chem.* **1992**, *267*, 12655–12659.

CT1003934